QUARKS-2024
XXII INTERNATIONAL SEMINAR ON HIGH-ENERGY PHYSICS

# Rotation Accounting and Black Hole Shadows

Stanislav Alexeyev, Artem Baiderin, Oleg Zenin

*Sternberg Astronomical Institute & Physics Faculty*
*Lomonosov Moscow State University*

RSF Russian Science Foundation
Supported by RSF via grant № 23-22-00073

# Constraints on gravity models from black hole shadows

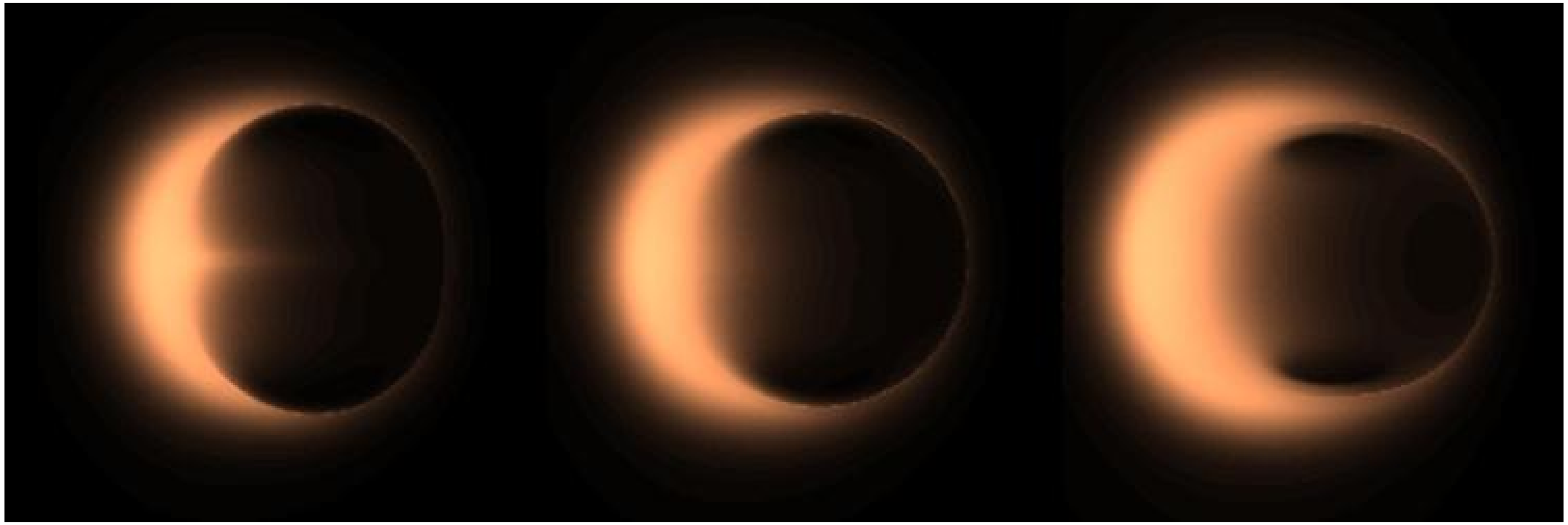

*Pic is taken from* https://www.eso.org/public/images/shadow-evt/

$$ds^2 = \left(1 - \frac{2M}{r} + \frac{Q^2}{r^2}\right)dt^2 - \frac{dr^2}{\left(1 - \frac{2M}{r} + \frac{Q^2}{r^2}\right)} - r^2 d\Omega^2$$

$$ds^2 = \frac{\Delta}{\rho^2}\left(dt - a\sin^2\theta d\tilde{\varphi}\right)^2 - \frac{\sin^2\theta}{\rho^2}\left((r^2 + a^2)d\tilde{\varphi} - adt\right)^2 - \frac{\rho^2}{\Delta}dr^2 - \rho^2 d\theta^2$$

A.Zakharov, **Phys. Rev. D,** Vol.90, P.062007 (2014) ... СА, А.А Байдерин, А.В. Немтинова, О.И. Зенин, ЖЭТФ 165, 508 (2024) arXiv 2404.16079

## Schwarzschild BH shadow

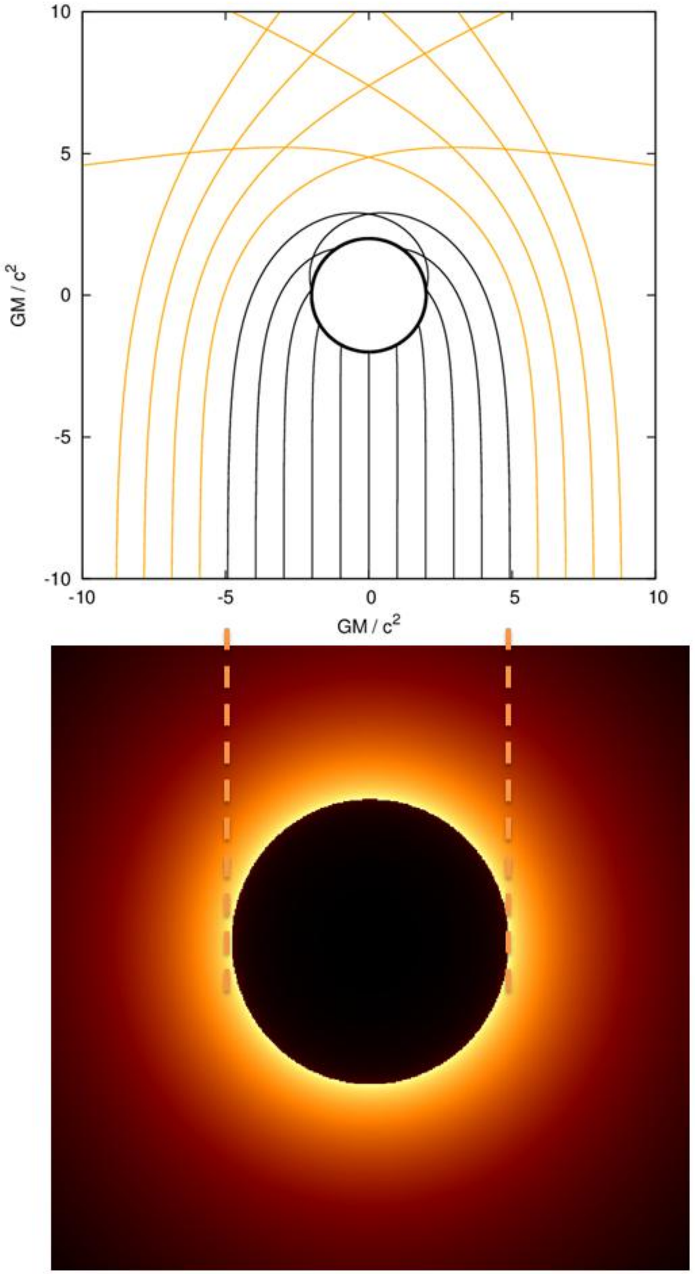


## Kerr BH shadow

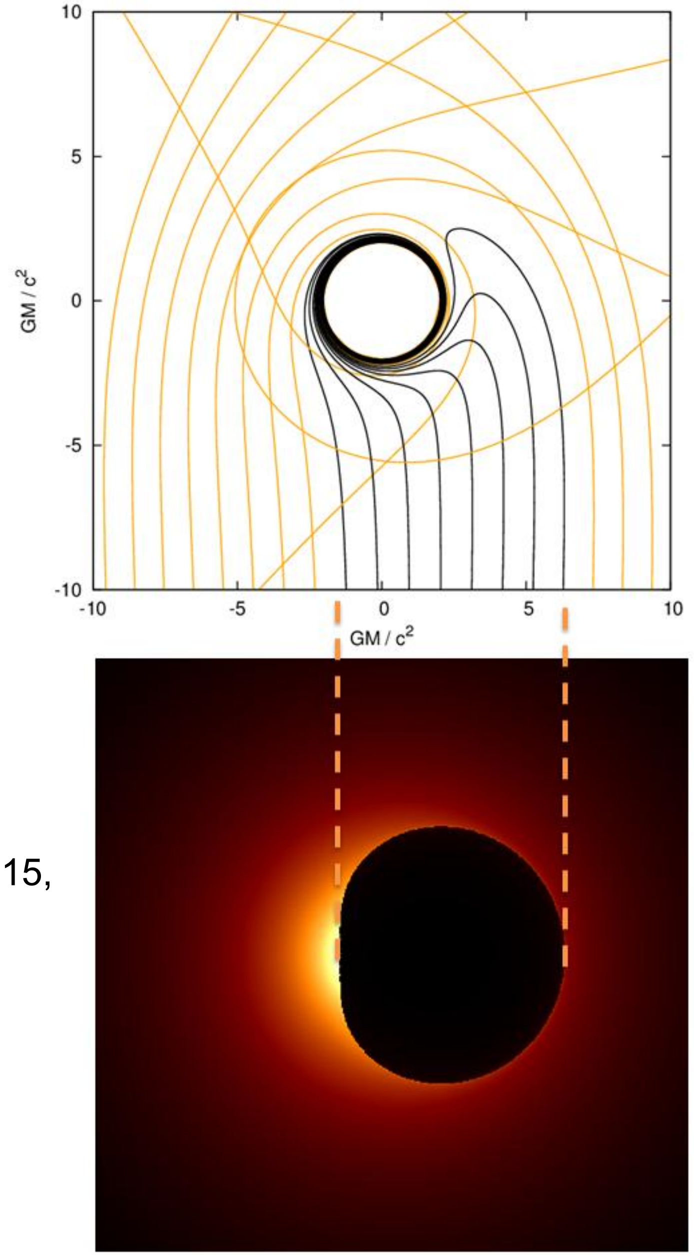


The most probable values of the rotation parameter and inclination of the rotation plane in BH:

M87*:
$a = 0.9375$[1]
Sgr A*:
$a = 0.5$ or $a = 0.94$
and $\theta = \pi/6$[2]

[2] Cui, Y.; others, Nature 621, 711–715, (2023).

[1] Akiyama, K.; others, Astrophys. J. Lett. 930, L13, (2022).

*Pic is taken from https://odysseyedu.wordpress.com/black-hole-shadow/*

# Horndesky theory

$$ds^2 = -\left(1 - \frac{2M}{r} - \frac{8\alpha_5\eta}{5r^3}\right)dt^2 + \frac{1}{1 - \frac{2M}{r} - \frac{8\alpha_5\eta}{5r^3}}dr^2 + r^2 d\Omega^2.$$

$$g_{tt} = -\left(1 - \frac{2Mr}{\rho^2} - \frac{8\alpha_5\eta}{5r}\right),$$

$$g_{t\phi} = -\frac{2a\sin^2\theta}{5r\rho^2}\left(4\alpha_5\eta + 9Mr^2\right),$$

$$g_{rr} = \rho^2\left(-\frac{8\alpha_5\eta}{5r} + a^2 - 2Mr + r^2\right)^{-1},$$

$$g_{\theta\theta} = \rho^2,$$

$$g_{\phi\phi} = \frac{\sin^2\theta}{\rho^2}\Bigg(r^4 + 2ar^2\cos^2\theta + a^4\cos^4\theta$$

$$+ \frac{8a^2\alpha_5\eta\sin^2\theta}{5r} + 2aMr\sin^2\theta + a^2r^2\sin^2\theta$$

$$+ a^4\cos^2\theta\sin^2\theta\Bigg),$$

SA, A.Baiderin, O.Zenin, submitted to EPJ C

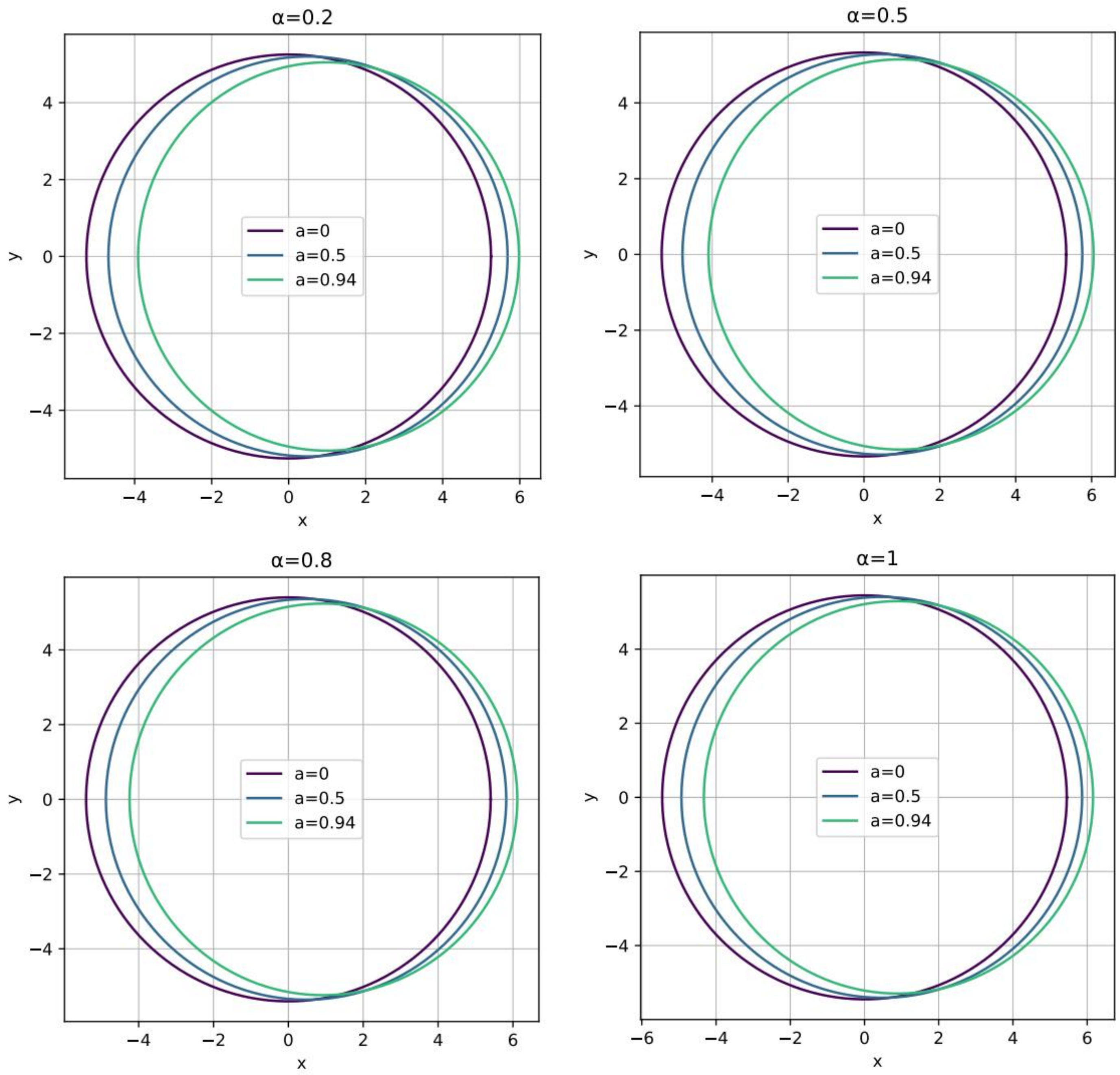


# Horndesky theory

SA, A.Baiderin, O.Zenin, submitted to EPJ C

# Horndesky theory

## The dependence of the shadow size against rotation **a**

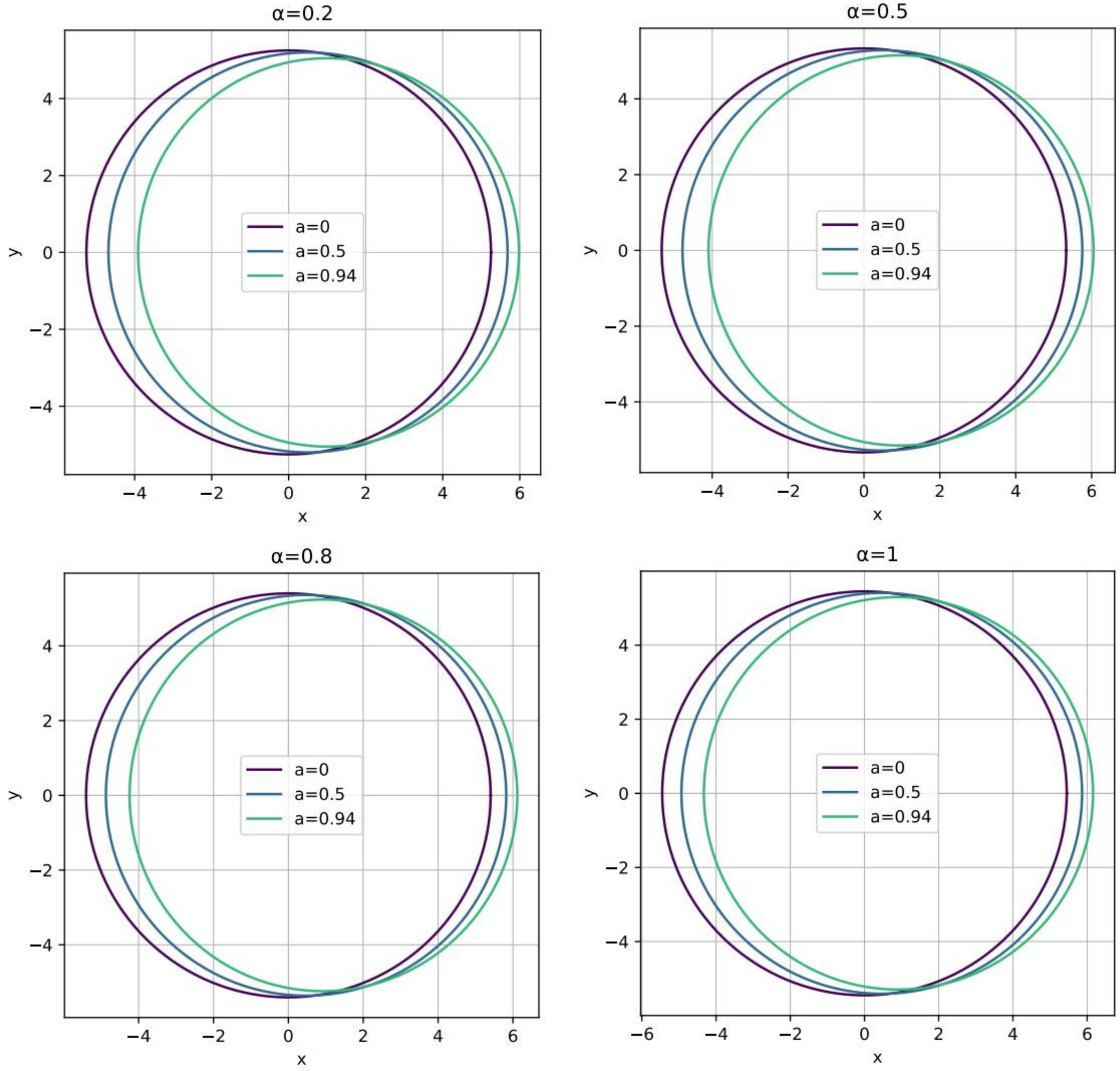


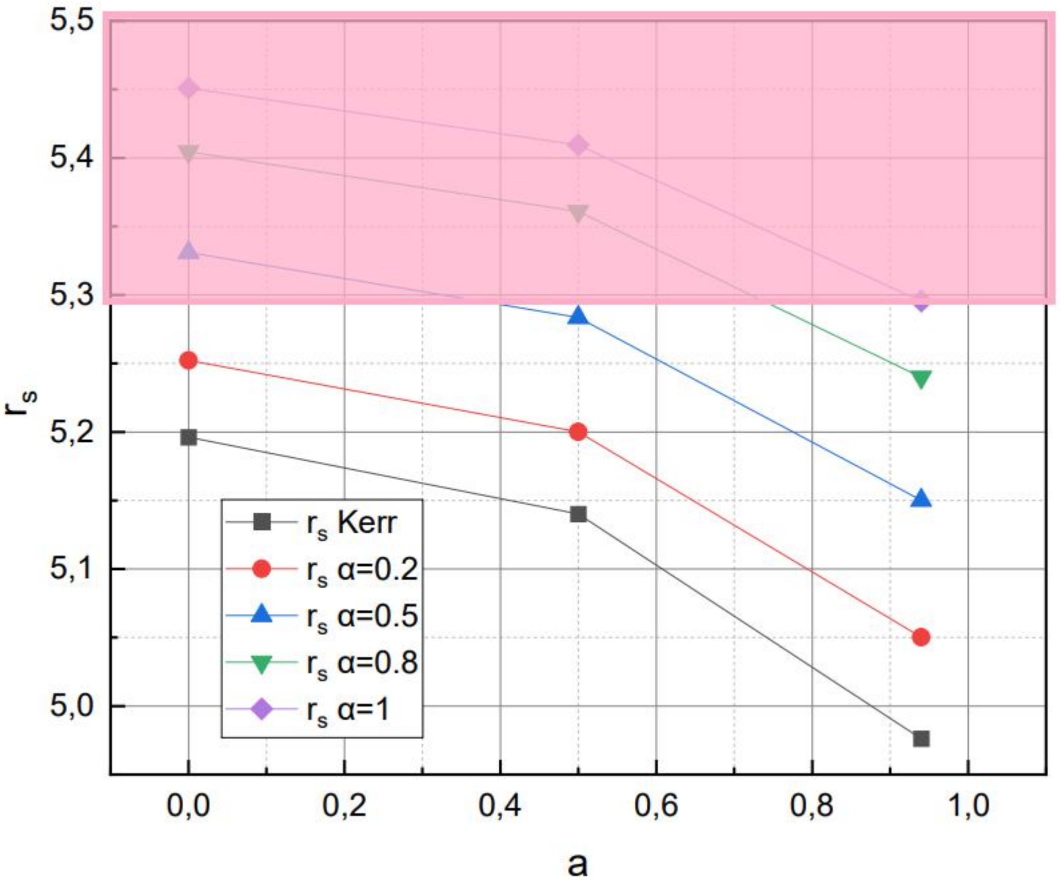


SA, A.Baiderin, O.Zenin, submitted to EPJ C

# Horndesky theory

## The dependence of shift (up case) and distortion (down case) against rotation a

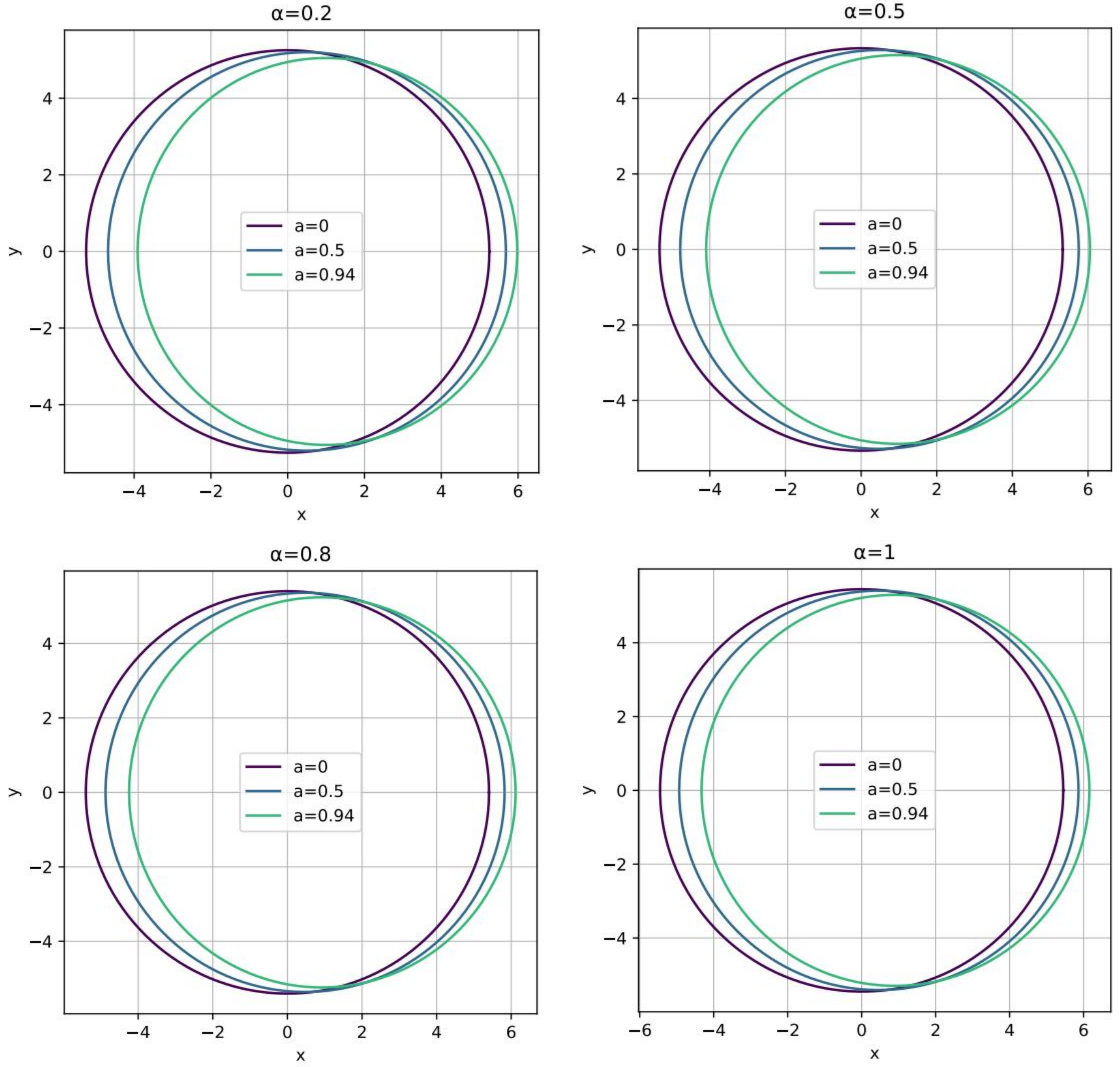


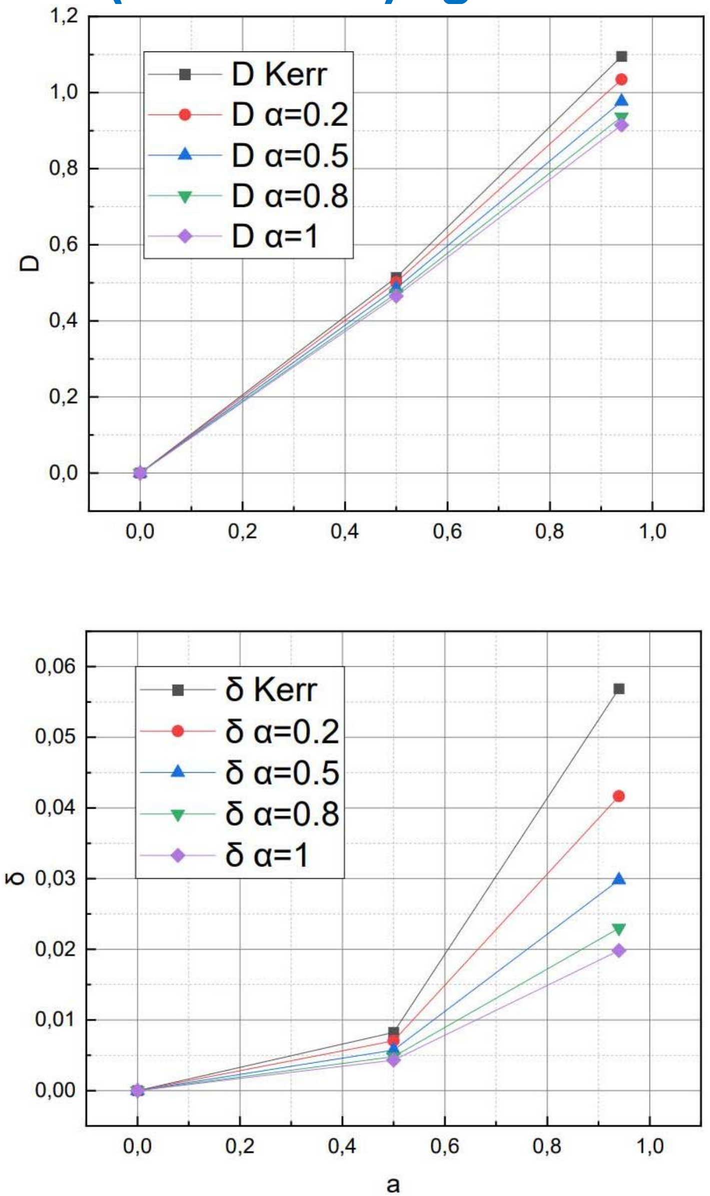


SA, A.Baiderin, O.Zenin, submitted to EPJ C

# Bumblebee model

$$ds^2 = -(1-\frac{2M}{r})dt^2 + \frac{1+l}{1-\frac{2M}{r}}dr^2 + r^2 d\Omega^2,$$

$$g_{tt} = \frac{r^{-1+\sqrt{1+l}}AB}{\sqrt{1+l}CD},$$

$$g_{t\phi} = -\frac{ar^{-l+\sqrt{1+l}}EB\sin^2\theta}{(1+l)CD},$$

$$g_{rr} = -\frac{(1+l)r^{-l+\sqrt{1+l}}B}{CG},$$

$$g_{\theta\theta} = r^{1+\sqrt{1+l}} + \frac{a^2(-4+8\sqrt{1+l})r^{-l+\sqrt{1+l}}\cos^2\theta}{8-2(1+\sqrt{1+l})},$$

$$g_{\phi\phi} = \frac{r^{-l+\sqrt{1+l}}\sin^2\theta(B+5a^2\cos^2\theta)}{(1+l)CD} \times (D(1+l) - Ka^2\cos^2\theta),$$

$$A = (2Mr^{1+l} - r^{1+\sqrt{1+l}} - a^2\cos^2\theta - a^2 l\cos^2\theta),$$

$$B = -3r^2 + \sqrt{1+l}r^2 - 3a^2\cos^2\theta - 4a^2\sqrt{1+l}\cos^2\theta,$$

$$C = -3 + \sqrt{1+l},$$

$$D = r^2 + a^2\sqrt{1+l}\cos^2\theta,$$

$$E = -r^2 - lr^2 - 2\sqrt{1+l}Mr^{\sqrt{1+l}} + \sqrt{1+l}r^{1+\sqrt{1+l}},$$

$$G = a^2 + a^2 l - 2Mr^{1+l} + r^{1-\sqrt{1+l}},$$

$$F = -2Mr^{\sqrt{1+l}} + r^{1+\sqrt{1+l}} - a^2 l\cos^2\theta,$$

$$K = \sqrt{1+l}F - r - 2lr^2 - D.$$

Casana, R.; Cavalcante, A.; Poulis, F.P.; Santos, E.B. Phys. Rev. D 97, 104001, (2018)  SA, A.Baiderin, O.Zenin, submitted to EPJ C,
S.Capozziello, S.Zare, H.Hassanabadi, e-Print: 2311.12896

# Bumblebee model

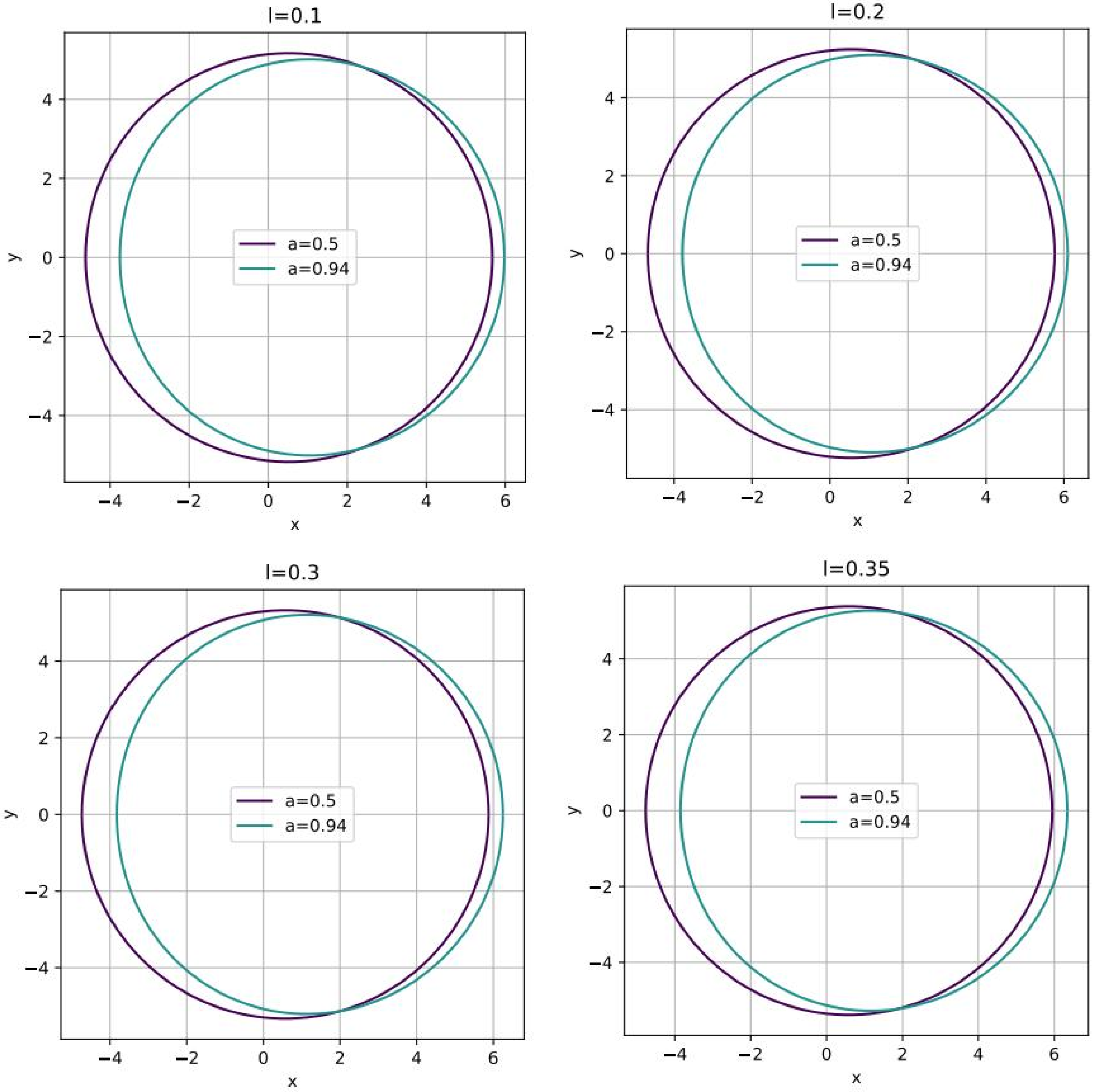


SA, A.Baiderin, O.Zenin, submitted to EPJ C

# Bumblebee model

## The dependence of the shadow size against rotation **a**

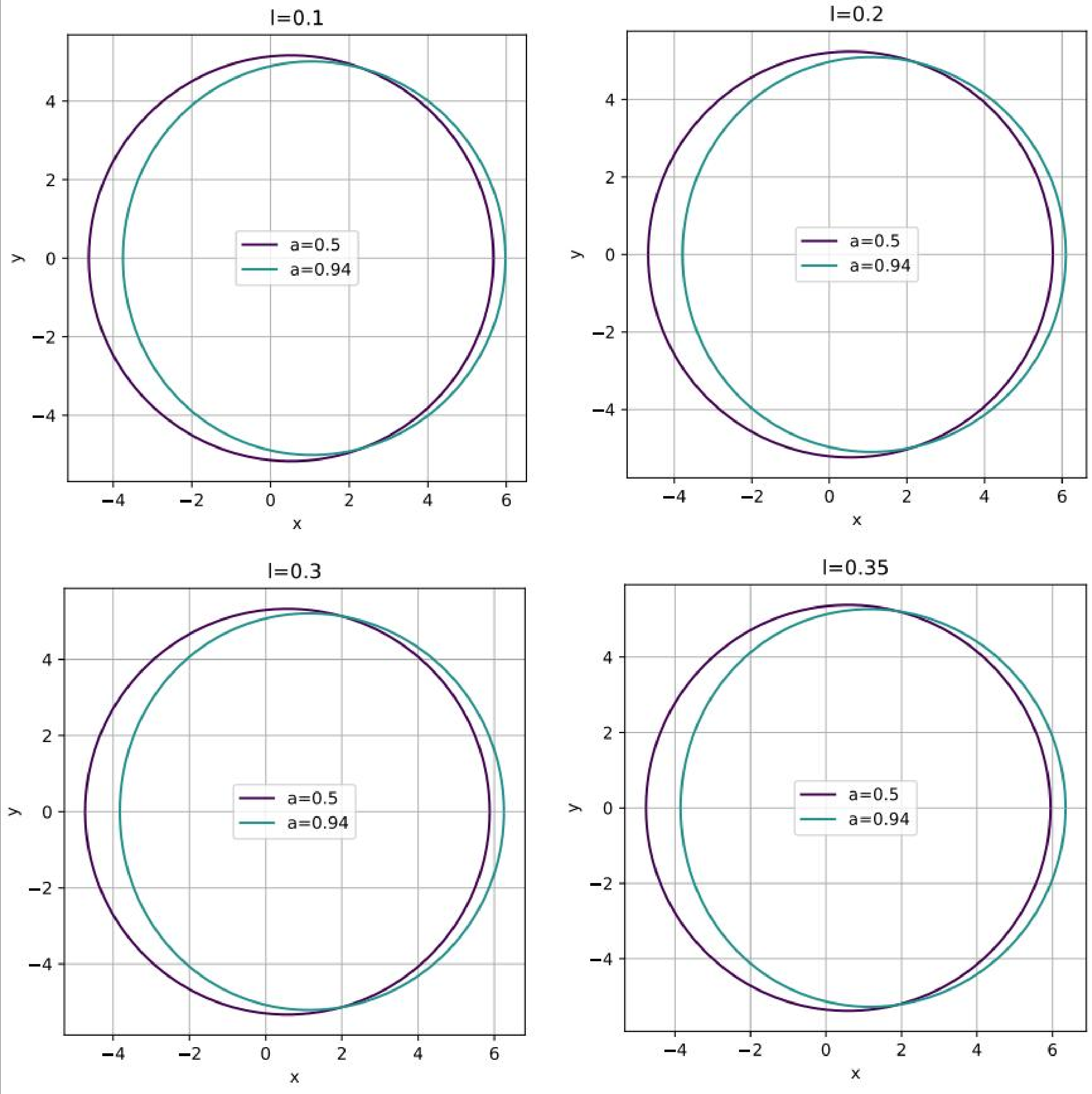


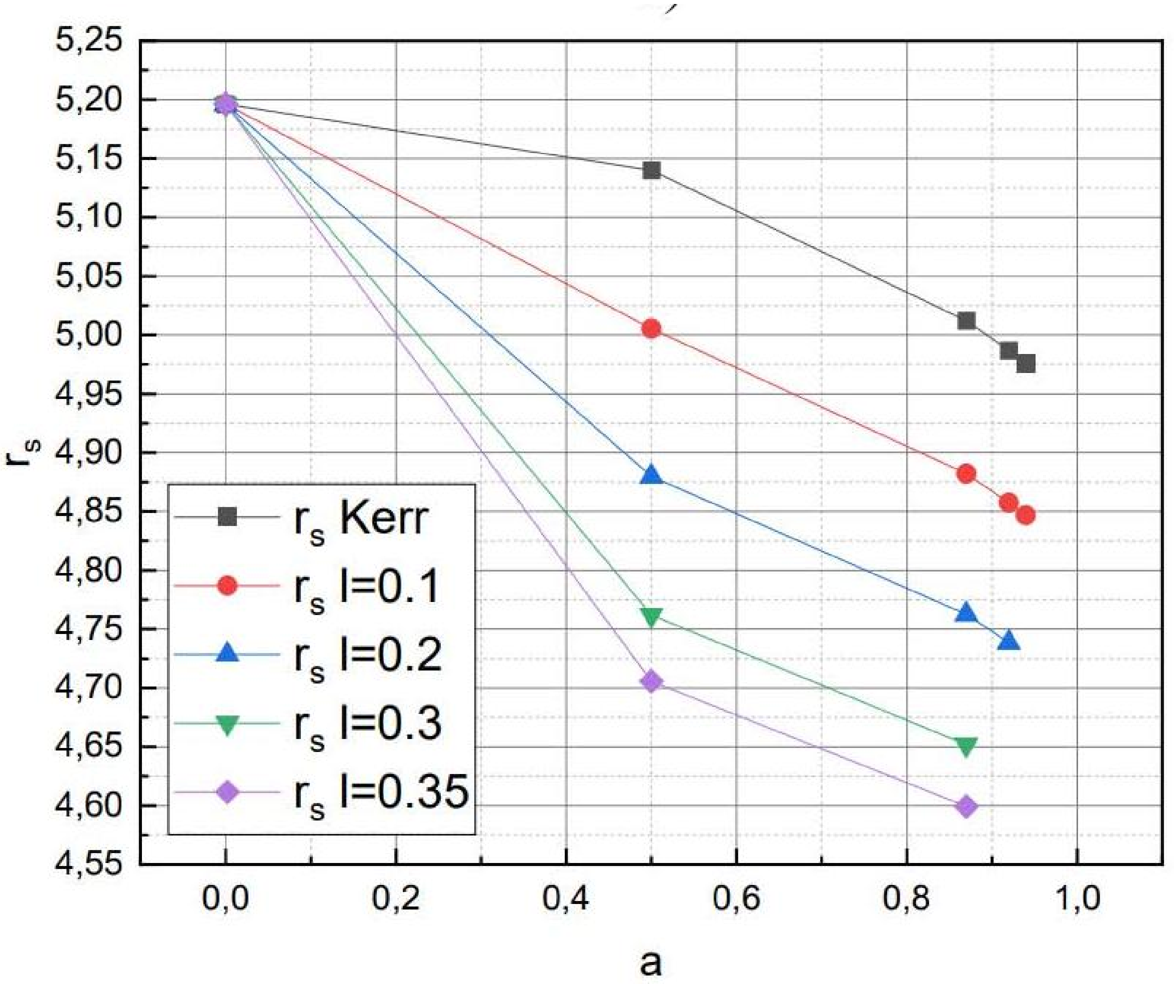


SA, A.Baiderin, O.Zenin, submitted to EPJ C

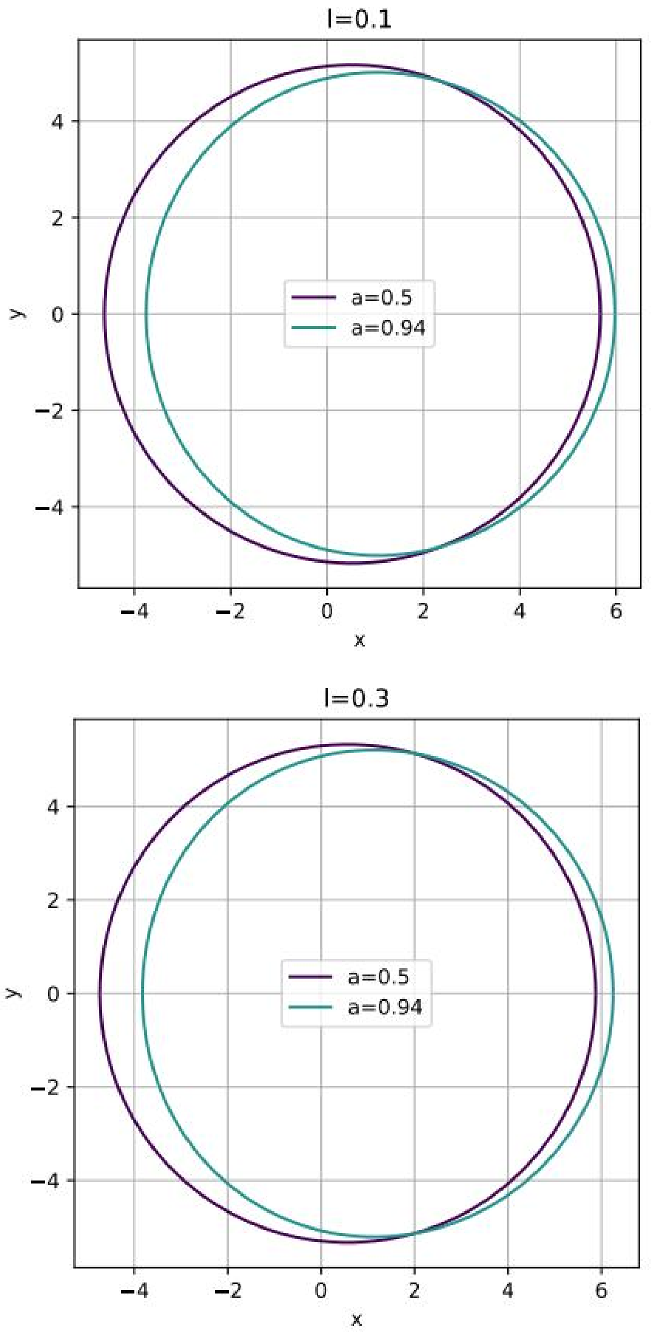


# Bumblebee model

## The dependence of shift (up case) and distortion (down case) against rotation **a**

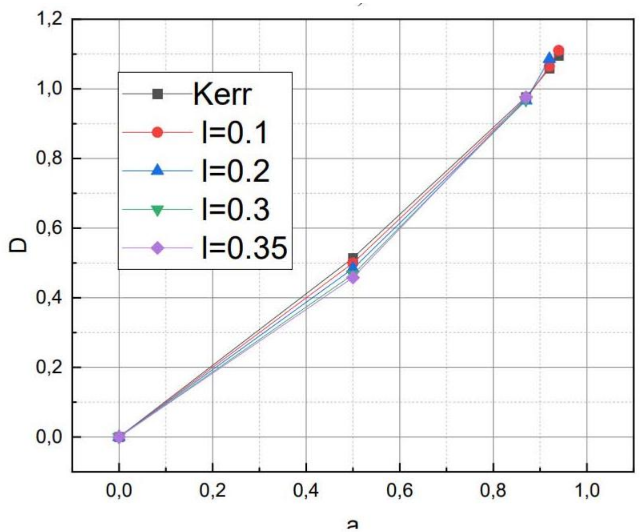


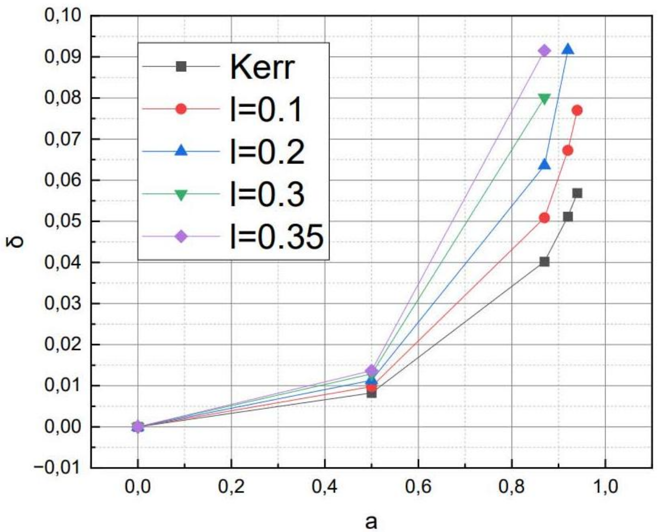


SA, A.Baiderin, O.Zenin, submitted to EPJ C

# Scalar Gauss-Bonnet Gravity

$$ds^2 = - f_s(1+\frac{\xi}{3r^3 f_s})dt^2 + \frac{(1-\frac{\xi}{r^3 f_s})}{f_s}dr^2 + \\ + (r^2 + \frac{\xi}{3r} + \frac{2\xi M}{3r^2})d\Omega^2,$$

$$g_{tt} = \frac{r^2(E+F\cos^2\theta)}{AB},$$
$$g_{t\phi} = -\frac{aCD\sin^2\theta}{AB},$$
$$g_{rr} = -\frac{AB}{r^2(E+F)},$$
$$g_{\theta\theta} = \frac{B}{3r^2},$$
$$g_{\phi\phi} = \frac{1+Q+9a^4r^4A\cos^4\theta+6a^2r^2G\sin^2\theta}{3r^2AB} + \frac{9a^4r^4A\cos^2\theta\sin^2\theta}{3r^2AB}.$$

$$A = \xi + 2Mr^2 - r^3,$$
$$B = 2\xi M + \xi r + 3r^4 + 3a^2r^2\cos^2\theta,$$
$$C = 2\xi M + \xi r + 3r^4,$$
$$D = A + 16M^2r^2 - 16Mr^4 + 4r^5,$$
$$E = 32\xi M^3 r - 16\xi M^2r^2 - 8\xi Mr^3 + 4\xi r^4 + 48M^2r^5 - 48Mr^6 + 12r^7,$$
$$F = -3a^2\xi - 6a^2Mr^2 + 3a^2r^3,$$
$$G = 16\xi M^3r^5 + 2\xi r^6 + 24M^2r^7 - 24Mr^8 + 6r^9,$$
$$K = 2\xi^2M + \xi^2r + 4\xi M^2r^2 + 2\xi r^4 + 6Mr^6 - 3r^7,$$
$$Q = 4\xi^3M(M+r) + \xi^2r^2(\xi + 2M^3 + 4M^2r + 10Mr^2 + 5r^3) + 3\xi r^6(8M^2+r^2) + 9r^{10}(2M-r).$$

SA, A.Baiderin, O.Zenin, submitted to EPJ C

# Scalar Gauss-Bonnet Gravity

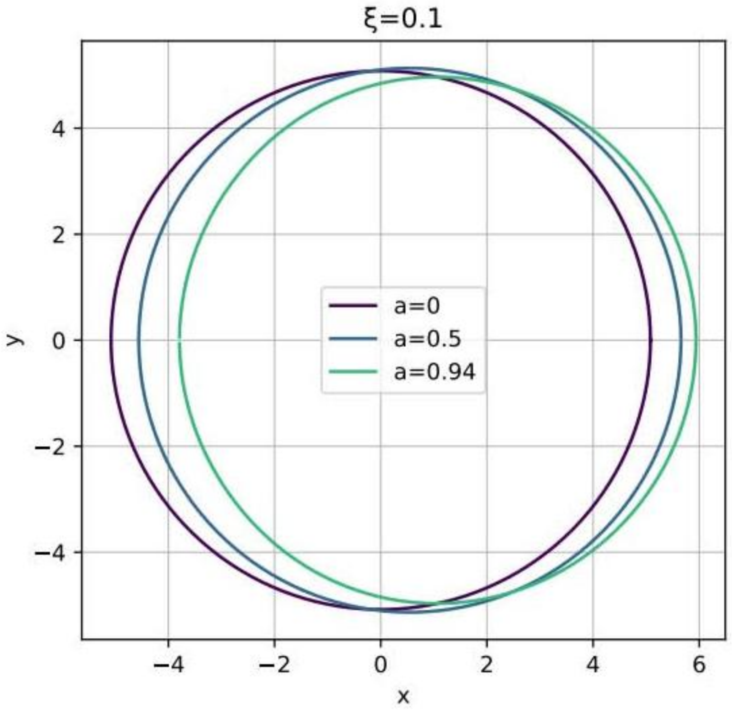


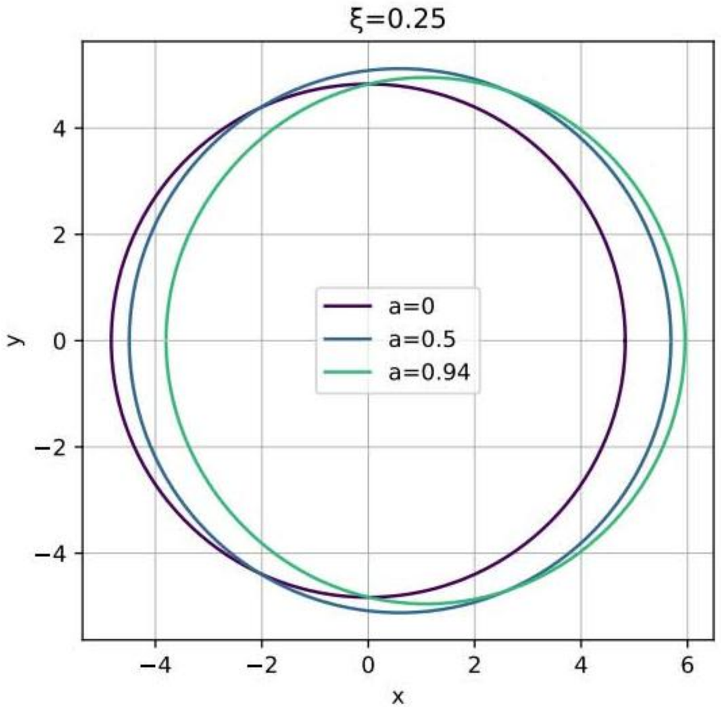


SA, A.Baiderin, O.Zenin, submitted to EPJ C

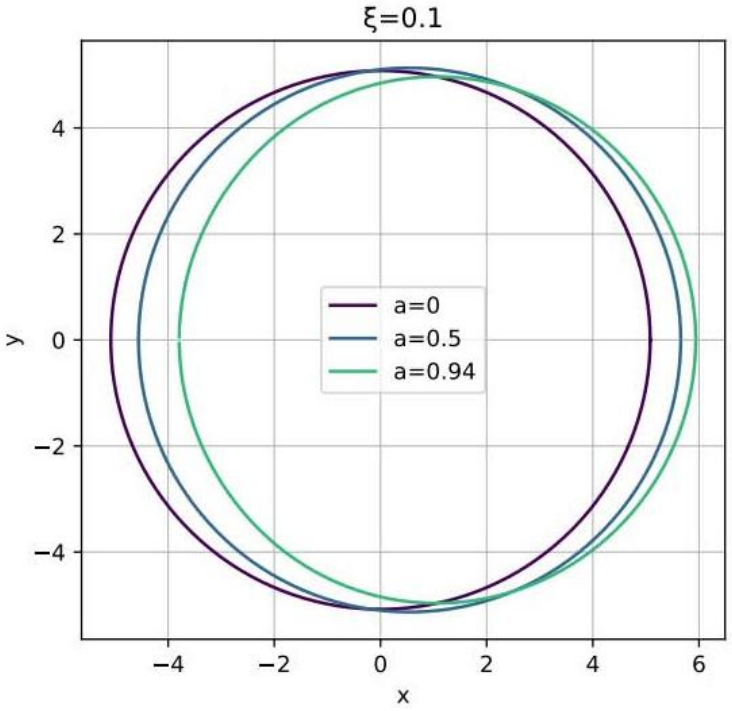


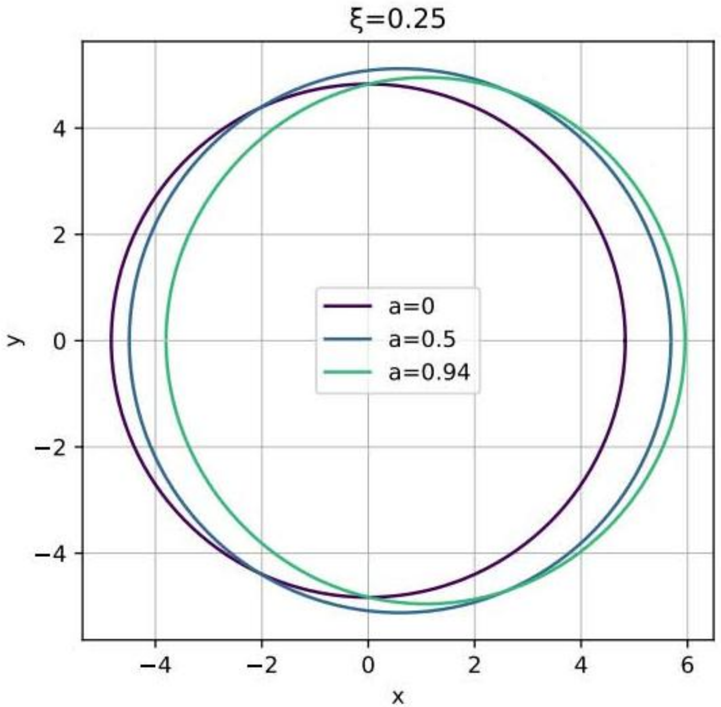


# Scalar Gauss-Bonnet Gravity

## The dependence of the shadow size against rotation **a**

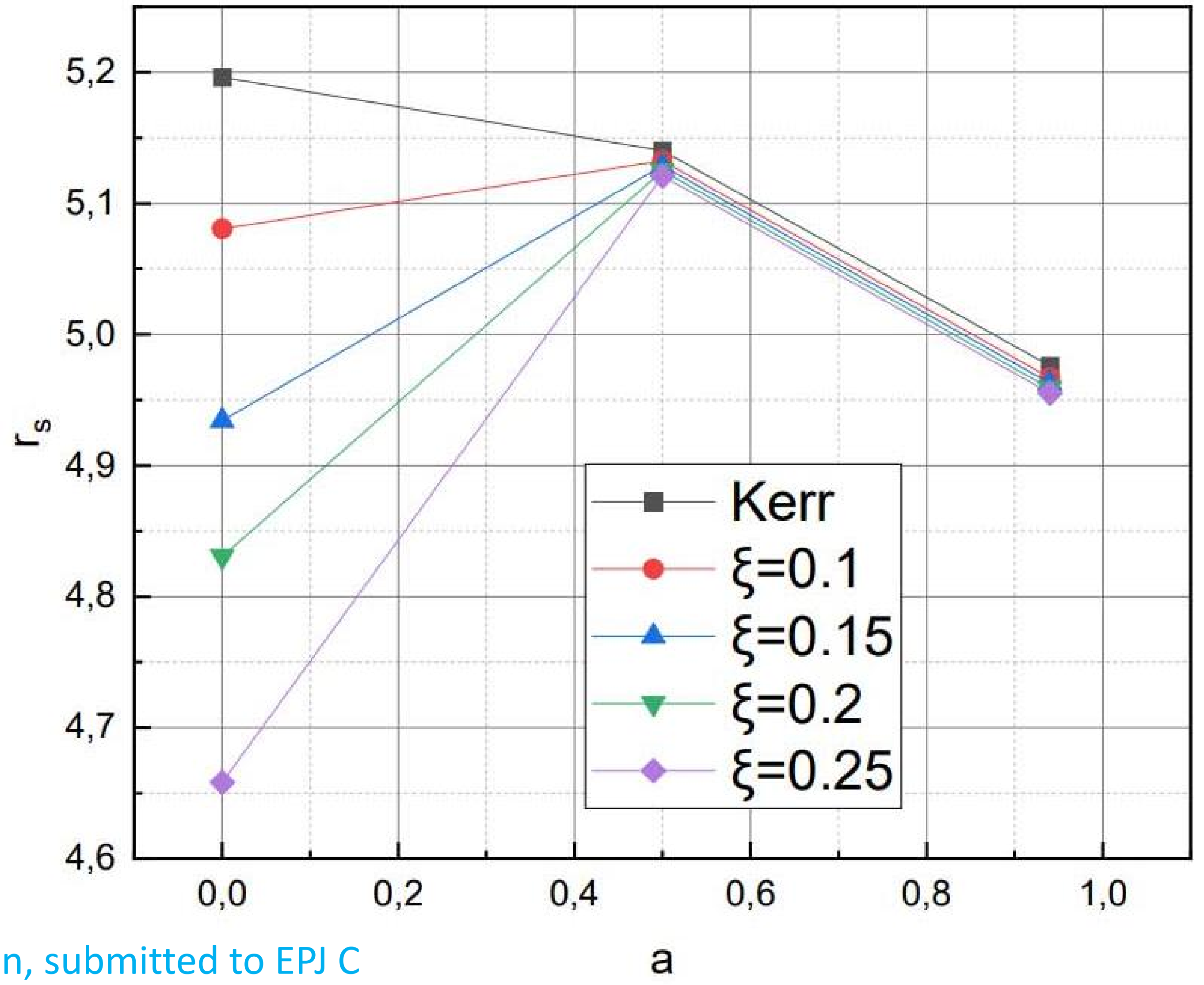


SA, A.Baiderin, O.Zenin, submitted to EPJ C

# Scalar Gauss-Bonnet Gravity

## The dependence of shift (up case) and distortion (down case) against rotation **a**

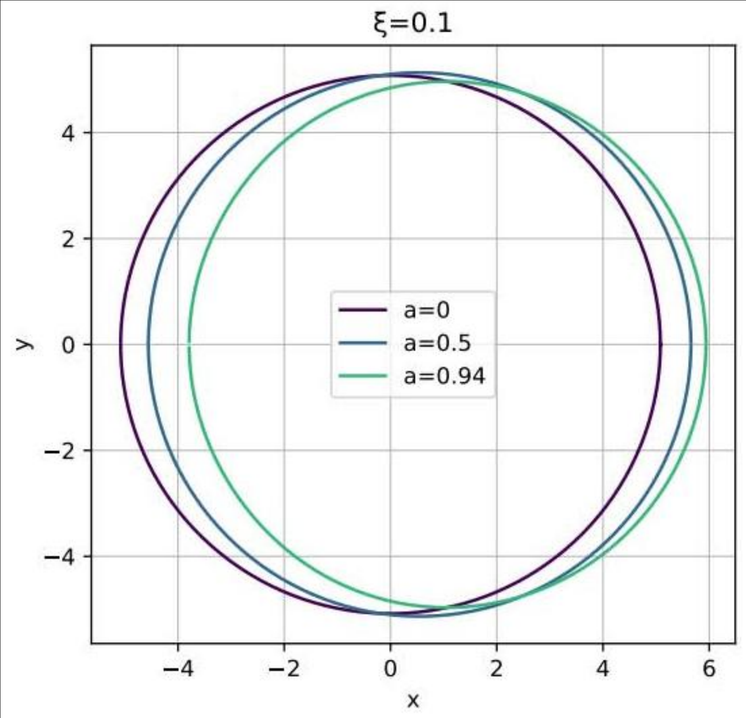


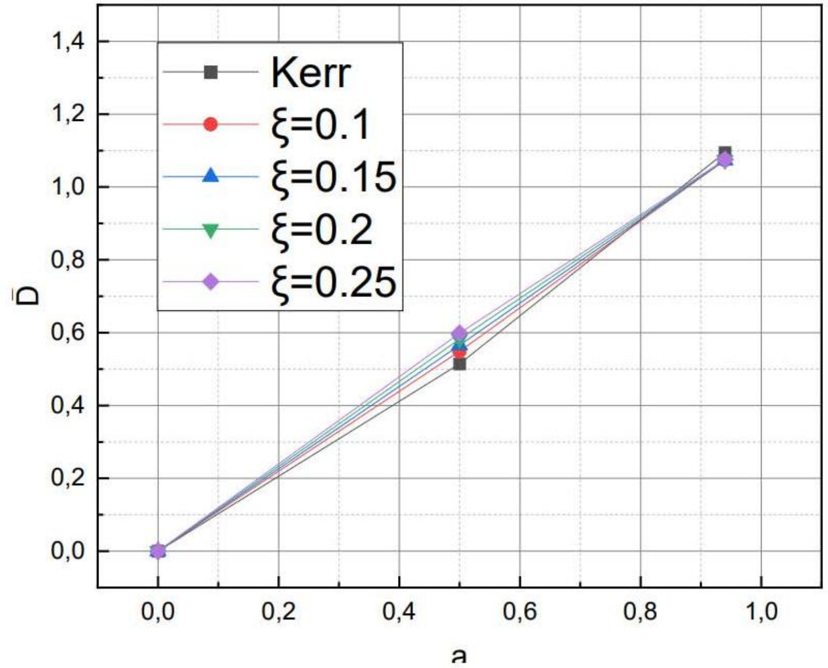


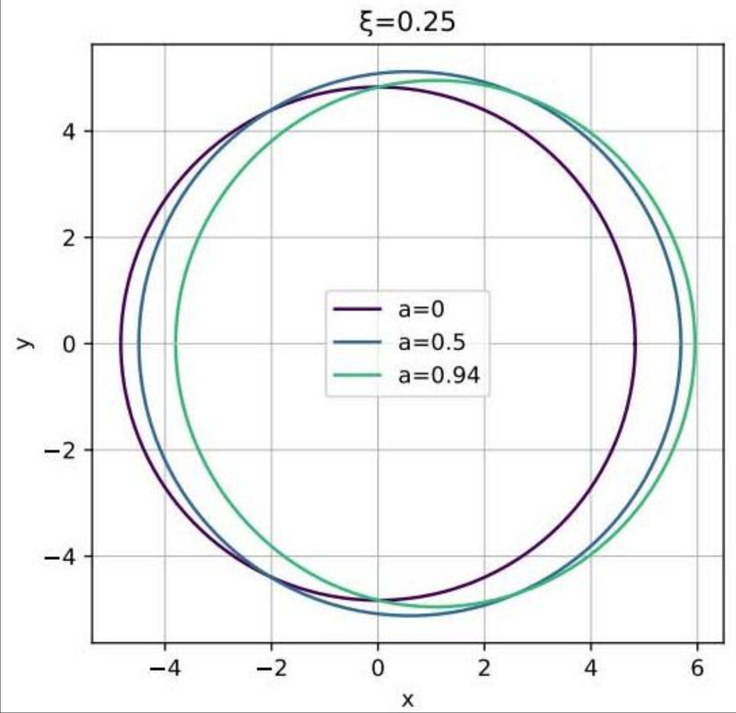


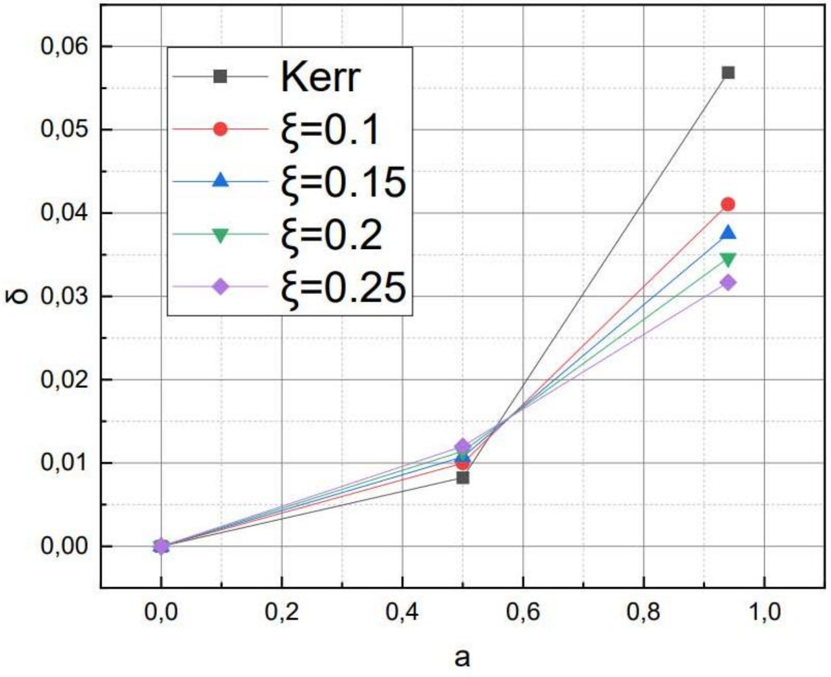


SA, A.Baiderin, O.Zenin, submitted to EPJ C

# Conclusions

We apply the most probable configurations for Sgr A*. Using the constrains on effective shadow size obtained by EHT the values α > 0.5 at a=0.5 for Horndesky model were excluded. In contrast for the fast rotation at a=0.94 all the configurations appear to be allowed. The shadow distortion differs from Kerr one very little for a=0.5. For a=0.94 it becomes less during α growing (from 5.5% at Kerr case till 2% at α=1). So the additional parameter acts opposite to rotation making its influence less.

For bumblebee model all the configurations appeared to be acceptable. For each l its own critical value of a exists ==> the fast rotation with a=0.94 is excluded for most range of l values. In contrast to the previous case the distortion grows when l becomes larger (up to 9.2% for l=0.2 and l=0.35). So in bumblebee model the additional parameter enhances the rotational effect.

In Gauss-Bonnet scalar gravity the shadow size has minor differences from Kerr case in contrast to the static case where the difference greater even for small values of coupling parameter (ξ=0.3 is maximally possible value). Analogously to bumblebee model all the configurations are allowed. For a=0.5 the distortion is greater than in pure Kerr case but for a=0.94 the distortion appears to be less (from 3.2% at ξ=0.25). So the theory weakens the effect of rotation.

Generally for three considered models two of them (Horndesky model and Gauss-Bonnet scalar gravity) weaken the effect of rotation and bumblebee model enhances it.

This conclusion matches the previous one at non-local gravity models study: extended gravity theories by themselves correct the effect of rotation in both directions. This fact seems to be important as the accuracy of shadow images permanently increases.

# Thank you for your atention!

RSF | Russian Science Foundation

Supported by RSF via grant № 23-22-00073